

Charge-response of the Majorana toric code

Ananda Roy and Fabian Hassler

JARA Institute for Quantum Information, RWTH Aachen University, 52056 Aachen, Germany

At zero temperature, a two dimensional lattice of Majorana zero modes on mesoscopic superconducting islands has a topologically ordered toric code phase. Recently, a Landau field theory has been proposed for the system that captures its different phases and the associated phase-transitions. It was shown that with the increase of Josephson tunneling between the islands, a continuous symmetry-breaking 3D-XY transition gets transformed into a discrete symmetry-breaking 3D-Ising transition through a couple of tricritical points and first order transitions. Using the proposed field theory, we analyze the charge-response of the system at the different continuous phase-transitions. We calculate the universal conductivity at the 3D-XY transitions and the change in the superconducting density at the Ising transition using $1/N$ expansion. Furthermore, by computing a one-loop correction to the field theory, we show that an additional tricritical point is likely to be present in the phase-diagram. Finally, we provide a mean-field calculation that supports the earlier proposed field theory.

I. INTRODUCTION

One of the most promising platforms for fault-tolerant quantum computation¹ is the toric code proposed by Kitaev.²⁻⁴ The ground space of the toric code is four-fold degenerate where two qubits can be encoded. The primary advantage of this way of encoding is that the degeneracy of the ground space depends only on the topology of the space on which the toric code is implemented and thus, is robust towards local perturbations. A direct realization of the toric code is by placing qubits on the links of a large square lattice with periodic boundary conditions and performing measurements that project the system to the topologically ordered ground space.² Alternately, a Hamiltonian can be designed whose the low-energy sector can be described by the toric code Hamiltonian.^{3,5} This is the case for a system of spins located at the edges of a 2D honeycomb lattice, interacting via alternating $\sigma_x\sigma_x$, $\sigma_y\sigma_y$ and $\sigma_z\sigma_z$ interactions around each plaquette of the lattice. For a suitable choice of interaction strengths, the system is in the toric code phase.³

In contrast to the aforementioned schemes of realizing the toric code using spins/qubits, alternative approaches have been proposed using Majorana zero modes.⁶⁻¹² In these approaches, a 2D lattice of mesoscopic superconducting islands is considered. On each of these islands, two Kitaev wires¹³ are embedded which contain localized Majorana zero modes. Due to the finite size, each island has a finite charging energy, denoted by $E_C = e^2/2C$, where C is the capacitance of each island to a ground plane. Due to the Josephson effect, the Cooper-pairs tunnel between different neighboring islands at a rate E_J . Furthermore, the Majorana zero modes enable tunneling of single electrons between two neighboring islands at a rate E_M .¹⁴ For vanishing Josephson tunneling rate and $E_M \ll E_C$, the system is in the topologically ordered toric code phase.^{6,10} Upon increasing the single-electron tunneling rate, the system undergoes a topological phase-transition of 3D-XY type into a topologically

trivial state.⁶ Moreover, in the limit of infinite Cooper-pair tunneling rate, the system is also in the toric code phase. In this case, the phase-transition to the topologically trivial state is of 3D-Ising type. A Landau field theory analysis for the system has been done in Ref. 15. It was shown that upon increasing the Josephson coupling strength from zero, the line of the 3D-XY topological phase-transition terminated at a 3D-XY tricritical point. Subsequently, it turned first order, which then terminated at a 3D-Ising tricritical point. Further increase of the Josephson coupling made the phase-transition a 3D-Ising one. The charge signatures of the different phases are as follows. For $E_J \ll E_M \ll E_C$, the system is a Mott-insulator. Upon increasing E_J , the system undergoes an additional 3D-XY phase-transition into a charge- $2e$ superconductor.¹⁶⁻²⁰ Most importantly, the system stays in the toric code phase both as a Mott-insulator and as a charge- $2e$ superconductor. Upon increasing E_M from either one of these phases, the system makes a topological phase-transition to a charge- e superconductor²¹⁻²³. Depending on the strength of E_J , it is the nature of this phase-transition that changes from 3D-XY to 3D-Ising.

Given that the phases have distinct charge signatures, we investigate the charge response across the different phase transitions. Measurement of the superconducting densities and correlation lengths reveals the critical exponents.¹⁵ Most importantly, a measurement of the electrical conductivity provides a unique signature that distinguishes between the different phase-transitions. The main goal of this work is to provide quantitative predictions of the conductivity that are amenable to experimental verification.

In the context of the Bose-Hubbard model at zero temperature, the conductivity at a 3D-XY transition has been shown to be a universal value. This conductivity value has been computed numerically using Monte-Carlo methods²⁴ and analytically using $1/N$ expansion²⁴ and ϵ expansion²⁵. These results can be directly applied to the two 3D-XY transitions and the 3D-XY tricritical point of our model. However, for the Ising transition and the Ising

tricritical point, a fresh computation is necessary. This computation is nontrivial due to the fact that the current is carried by two coupled Ising degrees of freedom, out of which only one undergoes the phase transition. We do this computation to leading order in the interaction using $1/N$ expansion. We show that as the system undergoes the transition from a charge- $2e$ to a charge- e superconductor, there is a jump in the superconducting density. In contrast to the 3D-XY transitions, there is no dissipative component to the conductivity.

In addition, we compute a one-loop correction to the field theory describing the system's transition from a Mott-insulator to a charge- $2e$ superconductor. This calculation indicates that another tricritical point of a 3D-XY type is likely to be present in the phase diagram. Lastly, we also perform a mean-field analysis of the model that provides additional support to the Landau field theory proposed in Ref. 15. Throughout this work, we restrict ourselves to zero temperature.

The paper is outlined as follows. First, we describe the basic building block of our model, Majorana zero modes on mesoscopic superconducting islands, in Sec. II. Then, we describe the microscopic Hamiltonian of the system in Sec. III. We map the problem to coupled spins and rotors, with nearest-neighbor interactions using Jordan-Wigner transformation in Sec. IV. We compute the one-loop correction to the field theory in Sec. V. We present the conductivity calculations in Sec. VI. We provide a concluding summary in Sec. VII. Finally, Appendix A contains the mean-field calculation.

II. SUPERCONDUCTING ISLANDS IN THE TOPOLOGICAL REGIME

In this section, we provide a concise summary of how charging effects can be consistently incorporated in the mathematical description of topological superconductors. We consider a toy model for a topological superconductor, the Kitaev wire.¹³ It describes the effect of coupling a quantum wire (modeled by a chain of spinless, fermionic modes) to an infinitely large superconductor. As the superconductor screens the charge of the electrons in the quantum wire, the relevant fermionic degrees at low energies are chargeless (Majorana) fermions.^{26,27} Even more interesting, in the topological phase of the Kitaev wire, Majorana zero modes, denoted by operators γ_a, γ_b , appear at its ends. These operators are Hermitian $\gamma_j = \gamma_j^\dagger$ and obey the Clifford algebra $\{\gamma_i, \gamma_j\} = 2\delta_{ij}$. Furthermore, the Majorana zero modes lead to a twofold degeneracy of the ground state. In a topological superconductor, these exotic degrees of freedom are in fact non-Abelian particles.^{28,29} As a result, topological superconductors realize a platform for topological quantum computation.^{30,31}

All these results essentially rely on the fact that the superconducting phase ϕ is a classical variable that has a well-defined value. The problem of extending the

results to a superconducting island with a fluctuating phase ϕ has been addressed, *e.g.*, in Refs. 6, 14, and 32. It has been shown that the connection between the neutral Majorana zero mode operators γ_a, γ_b and the charged electronic annihilation operator c is given by $c = e^{-i\phi/2}(\gamma_a + i\gamma_b)/2$.³³ Note that the charge on the superconducting island is carried by the Cooper-pairs in the condensate and thus, is measured by $Q = -2ei(d/d\phi)$ where $e > 0$ is the elementary charge. Thus, the process of removing an electron from the superconducting island (described by c) both flips the fermion parity $\mathcal{P} = -i\gamma_a\gamma_b$ (because of the action of $\gamma_a + i\gamma_b$) and removes a charge $-e$ from the island (because of the action of $e^{-i\phi/2}$). After all, fundamentally, the particles on the topological superconductor are electrons. So any physical state of the system has to be reachable by applying the electronic operators c, c^\dagger to the vacuum state without any particles present.

These arguments lead to the conclusion that the physical Hilbert space is not simply given by the tensor product $\mathcal{H}^\otimes = \mathcal{H}_\phi \otimes \mathcal{H}_\gamma$ of the condensate Hilbert space \mathcal{H}_ϕ (on which ϕ and Q act) and the Majorana Hilbert space \mathcal{H}_γ (on which γ_a and γ_b act). Instead, the states $\psi \in \mathcal{H}^\otimes$ are physical only if they are connected to the vacuum state by addition or removal of electrons. Counting the fermion parity, denoted by the operator \mathcal{P} , with the charge on the island, denoted by the operator Q , yields the constraint

$$(-1)^{Q/e}\psi = \mathcal{P}\psi. \quad (1)$$

All states in the physical Hilbert space have to fulfill this constraint. Therefore, in the case of a pair of Majorana zero modes on an island, even though the zero modes are chargeless, the two ground states $|\pm\rangle$ (that differ in fermion parity with $\mathcal{P}|\pm\rangle = \pm|\pm\rangle$) are not degenerate in energy. This is because they necessarily correspond to a different charging of the mesoscopic superconducting island: $Q \in \{0, 2e, 4e, \dots\}$ for the case of $\mathcal{P} = +$ and $Q \in \{e, 3e, 5e, \dots\}$ for the case of $\mathcal{P} = -$.

On first sight, it might appear that the finite charging energy of a mesoscopic superconducting island prevents any degeneracy due to the neutral Majorana zero modes. However, it can be easily seen that this conclusion is incorrect for the situation where there are two Kitaev wires and thus four Majorana zero modes $\gamma_a, \gamma_b, \gamma_c, \gamma_d$ on the island. In this case, the fermion parity constraint still is given by (1) but with a fermion parity operator $\mathcal{P} = -\gamma_a\gamma_b\gamma_c\gamma_d$ that involves all of the zero modes. In particular, we imagine to pair γ_a, γ_b (γ_c, γ_d) with the ground state degeneracy given by the two eigenvalues of the partial parity $\mathcal{P}_{ab} = i\gamma_a\gamma_b$ ($\mathcal{P}_{cd} = i\gamma_c\gamma_d$). In the Majorana sector, the ground state is four fold degenerate with the four states given by $|p_1, p_2\rangle = |p_1\rangle_{ab} \otimes |p_2\rangle_{cd}$, with $p_1, p_2 \in \{\pm\}$. As before, the finite charging energy will split states that correspond to different eigenvalues of the charge operator Q . However, in this case the constraint (1) only implies that the states with different total fermion parity \mathcal{P} are not degenerate. This leaves the de-

generacy of the set of states $\{|+, +\rangle, |-, -\rangle\}$ and of the set of states $\{|+, -\rangle, |-, +\rangle\}$. So even at finite charging energy, there is a finite topological degeneracy of the ground state remaining.³⁴

Physically, the degeneracy of the states $\{|+, -\rangle, |-, +\rangle\}$ can be understood due to the fact that a single unpaired electron can be moved from the fermionic mode ab to cd (or the other way round). As a result, the fermion parity on each of the two pairs changes without changing the charging energy. More interestingly, the degeneracy of the state $|+, +\rangle$ with $|-, -\rangle$ arises from the fact that starting with $|+, +\rangle$ the state $|-, -\rangle$ can be reached by breaking a Cooper pair and filling both the modes ab and cd . This process does not involve taking any charge to or from the island and thus, does not change the charge Q on the superconducting island. Note that due to the presence of the zero modes, one does not pay the usual superconducting energy gap to break the Cooper-pair.

A remaining question is how to describe the tunneling of single charges between two superconducting islands i, j . Note that in a multi-island situation the parity constraint (1) has to be fulfilled on each of the islands separately. For concreteness, let us assume that the zero modes d on island i is close to the mode a on island j . The resulting tunneling of single electrons leads to a term

$$H_{e\leftrightarrow e} \propto i\gamma_d^i \gamma_a^j \cos\left(\frac{\phi_i - \phi_j}{2}\right), \quad (2)$$

also dubbed 4π -periodic Josephson effect.¹³ It is easy to see that under the action of this Hamiltonian [Eq. (2)], the state still satisfies the constraint [Eq. (1)] both on island i and j . The reason is that while the cos-term adjusts the charge (by increasing it by e on one of the islands and decreasing it on the other island correspondingly), the factor $i\gamma_d^i \gamma_a^j$ flips the fermion parity on each side such that physical states are mapped onto physical states in this process.

III. MODEL HAMILTONIAN OF THE MAJORANA TORIC CODE

With this introduction, it can be seen that the Hamiltonian of the system depicted in Fig. 1 is given by $H = H_C + H_J + H_M$, where

$$\begin{aligned} H_C &= 4E_C \sum_i n_i^2, & H_J &= -E_J \sum_{\langle i,j \rangle} \cos(\phi_i - \phi_j), \\ H_M &= -E_M \sum_{\langle i,j \rangle} V_{i,j} \cos\left(\frac{\phi_i - \phi_j}{2}\right). \end{aligned} \quad (3)$$

Here, the superconducting phase ϕ_i and the excess charge $n_i = Q_i/2e$ (in units of Cooper pairs) on the i -th island are canonically conjugate. We treat the idealized case of zero offset charges in the absence of disorder. The

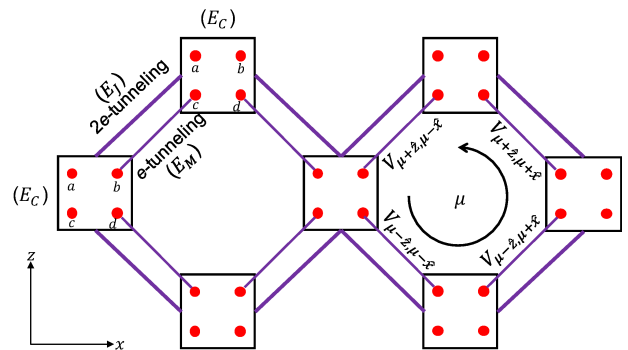


FIG. 1. (Color online) Schematic of two plaquettes of the lattice of Majorana zero modes (denoted by red dots) on superconducting islands (denoted by white squares).¹⁵ The three relevant energy scales are shown: the charging energy of each island E_C , the rate of tunneling of Cooper-pairs E_J (denoted by thick links) and the rate of tunneling of single-electrons E_M (denoted by thin links).

Majorana tunneling operator V_{ij} between the two neighboring islands i, j is given by (see Fig. 1)⁷

$$\begin{aligned} V_{\mu+\hat{z}, \mu-\hat{x}} &= i\gamma_c^{\mu+\hat{z}} \gamma_b^{\mu-\hat{x}}, & V_{\mu-\hat{z}, \mu-\hat{x}} &= i\gamma_a^{\mu-\hat{z}} \gamma_d^{\mu-\hat{x}}, \\ V_{\mu-\hat{z}, \mu+\hat{x}} &= i\gamma_c^{\mu+\hat{x}} \gamma_b^{\mu-\hat{z}}, & V_{\mu+\hat{z}, \mu+\hat{x}} &= i\gamma_a^{\mu+\hat{x}} \gamma_d^{\mu+\hat{z}}, \end{aligned} \quad (4)$$

where the γ_α^i are Hermitian operators. The fermion parity on the i -th island is given by the operator $\mathcal{P}_i = -\gamma_a^i \gamma_b^i \gamma_c^i \gamma_d^i$. As the charge is constrained by the fermion parity, the (physical) Hilbert-space for the Hamiltonian H is spanned by the wavefunctions satisfying $\psi(\phi_i + 2\pi) = e^{i\pi Q_i/e} \psi(\phi_i) = \mathcal{P}_i \psi(\phi_i)$ [cf. Eq. (1)].¹⁴ At finite charging energy, the ground state is in the even parity sector on each island ($\mathcal{P}_i \equiv +1$). In this sector, the four Majorana zero modes on each island encode one qubit³⁵ and, neglecting H_J , a perturbation calculation in E_M/E_C yields the toric code Hamiltonian.^{6,10}

IV. MAPPING TO A COUPLED SPIN-ROTOR HAMILTONIAN

In this section, we map the Hamiltonian to that of spins coupled to rotors using Jordan-Wigner transformation. Note that the Jordan-Wigner mapping presented in this section is different from the one presented in Ref. 7. Unlike the mapping of Ref. 7, the current one keeps the size of the Hilbert space invariant and thus, captures the degeneracies in the spectrum of the Hamiltonian.

First, we perform a gauge transformation in order to simplify the Hilbert-space to 2π -periodic functions.³⁶ This is done by applying a unitary transformation

$$H \rightarrow \Omega^\dagger H \Omega, \quad \psi \rightarrow \Omega^\dagger \psi \quad (5)$$

where

$$\Omega = \prod_i e^{iq_i \phi_i/2}, \quad q_i = \frac{1 - \mathcal{P}_i}{2}. \quad (6)$$

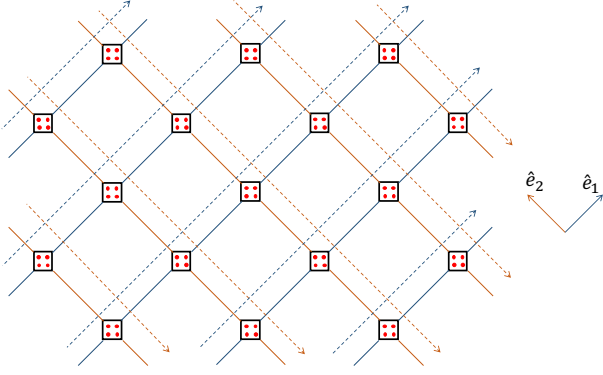


FIG. 2. (Color online) Schematic of the Jordan-Wigner transformation for the Majorana zero modes for an $L \times L$ lattice for both open and periodic boundary conditions.

As a result, now only 2π -periodic wavefunctions correspond to the physical states of the system. After the transformation, H_J stays invariant, while the H_C, H_M gets transformed as

$$H_C = 4E_C \sum_i \left(n_i + \frac{q_i}{2} \right)^2, \\ H_M = -\frac{E_M}{2} \sum_{\langle i,j \rangle} \left(e^{-iq_i \phi_i} V_{i,j} e^{iq_j \phi_j} + \text{H.c.} \right). \quad (7)$$

Next, we map the Majorana zero modes into spins using a Jordan-Wigner transformation. Consider an $L \times L$ lattice with periodic boundary conditions. Starting from any point on the lattice, we enumerate the Majorana zero modes traversing the lattice first in the \hat{e}_1 direction (along the blue arrows in Fig. 2). Once all the L lines along the \hat{e}_1 direction have been traversed, we do the same in the \hat{e}_2 direction (along the orange arrows in Fig. 2). Thus, each island is traversed twice, once in the \hat{e}_1 and then in the \hat{e}_2 direction. For the i^{th} -island, while traversing in the $\hat{e}_{1(2)}$ direction, the map \mathcal{M} maps the Majorana zero modes to spins as follows:

$$\mathcal{M}(\gamma_{2i_k-1}) = \left[\prod_{j=1}^{i_k-1} \sigma_j^z \right] \sigma_{i_k}^x, \\ \mathcal{M}(\gamma_{2i_k}) = \left[\prod_{j=1}^{i_k-1} \sigma_j^z \right] \sigma_{i_k}^y, \quad k = 1, 2. \quad (8)$$

Under this mapping, the fermion parity operator of the i^{th} -island is given by

$$\mathcal{P}_i = -\gamma_a^i \gamma_b^i \gamma_c^i \gamma_d^i = \gamma_{2i_1-1} \gamma_{2i_1} \gamma_{2i_2-1} \gamma_{2i_2} = \sigma_{i_1}^z \sigma_{i_2}^z. \quad (9)$$

Using Eqs. (4) and (8), for any link at the interior of the lattice (connecting sites i, j with neither i, j being a multiple of L), the $V_{i,j}$ are transformed as

$$V_{i_k, j_k} = \sigma_{i_k}^x \sigma_{j_k}^x, \quad k = 1, 2. \quad (10)$$

The interactions on the links at the boundary, where the lattice wraps around (connecting sites i, j with i or j being a multiple of L) are nonlocal. For instance, along the first line of enumeration, the interaction coupling the Majorana modes γ_{2L} and γ_1 is

$$V_{L,1} = \left[\prod_{i=1}^L \sigma_i^z \right] \sigma_1^x \sigma_L^x. \quad (11)$$

However, one can check that the product of the fermion parity along each of these lines is a conserved quantity.⁸ Thus, the Hilbert space splits into sectors where each of these $\prod_{i=1}^L \sigma_i^z = \pm 1$. In what follows, we will fix all these quantities to be $+1$. Similar analysis can be done for other choices. Naturally, for open boundary conditions, this nonlocal interaction does not arise. Thus, the thermodynamic properties are described by the interactions on-site and those mediated by the internal links.

Next, we reduce the effective Hilbert space size that the interaction Hamiltonian acts on. To that end, we lay down a Bell-basis for the spins on the i^{th} -island.⁷ We define a sign qubit (s) and a target qubit (t) on each island, whose joined state is given by $|\psi^{s,t}\rangle \equiv |s, t\rangle$:

$$|s=0, t=0\rangle = \frac{1}{\sqrt{2}}(|00\rangle + |11\rangle), \\ |s=0, t=1\rangle = \frac{1}{\sqrt{2}}(|01\rangle + |10\rangle), \\ |s=1, t=0\rangle = \frac{1}{\sqrt{2}}(|00\rangle - |11\rangle), \\ |s=1, t=1\rangle = \frac{1}{\sqrt{2}}(|01\rangle - |10\rangle). \quad (12)$$

Thus, s is the sign bit and the t is the two-qubit parity bit of information in the superposition. In this basis, the operators $\sigma_{i_k}^x, \sigma_{i_k}^z, k = 1, 2$ get mapped to:

$$\sigma_{i_1}^x |s, t\rangle = \sigma_{i_1, t}^x \sigma_{i_1, s}^z |s, t\rangle, \quad \sigma_{i_2}^x |s, t\rangle = \sigma_{i_2, t}^x |s, t\rangle, \\ \sigma_{i_1}^z |s, t\rangle = \sigma_{i_1, s}^z |s, t\rangle, \quad \sigma_{i_2}^z |s, t\rangle = \sigma_{i_2, t}^z \sigma_{i_1, s}^x |s, t\rangle, \quad (13)$$

where $\sigma_{i, s(t)}^x, \sigma_{i, s(t)}^z$ are the Pauli operators for the sign (target) qubits. Thus, the interaction Hamiltonian $\sigma_{i_1}^x \sigma_{j_1}^x$ along \hat{e}_1 direction gets mapped to an effective interaction between the target qubits where the sign of the interaction is determined by the σ_s^z eigenvalue of the sign qubits. We can define a classical bit s_{ij} on each link connecting the i^{th} and the j^{th} island in the \hat{e}_1 direction that is the product of the σ^z -eigenvalues of the corresponding sign qubits (cf. Fig. 3). The resultant interaction Hamiltonian, after a trivial rotation on the target qubits, is then written by (we drop the t -index on the spins for clarity)

$$H_C = 4E_C \sum_i \left(n_i + \frac{1 + \sigma_i^z}{4} \right)^2, \quad (14)$$

$$H_M = -\frac{E_M}{2} \sum_{\langle i,j \rangle} s_{i,j} \left\{ \sigma_i^- \sigma_j^- (e^{i\phi_i} + e^{i\phi_j}) \right. \\ \left. + \sigma_i^- \sigma_j^+ [1 + e^{i(\phi_i - \phi_j)}] + \text{H.c.} \right\},$$

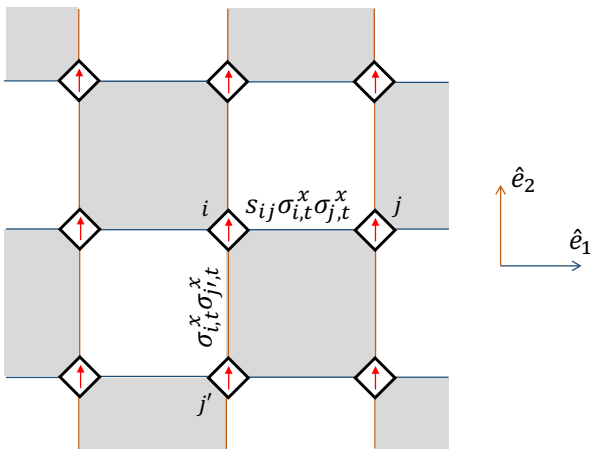


FIG. 3. (Color online) Schematic of an inner 3×3 block of the rotated lattice. The interaction between the i^{th} , j^{th} and the i^{th} , j'^{th} islands are shown after the Jordan-Wigner transformation in the Bell-basis. The interaction on the horizontal link (in the \hat{e}_1 direction) connecting the i^{th} and the j^{th} islands is given by $s_{ij} \sigma_{i,t}^x \sigma_{j,t}^x$, where s_{ij} is the product of the σ_s^z eigenvalues of the sign qubits on the corresponding islands. The interaction on the vertical link (in the \hat{e}_2 direction) between the i^{th} and the j^{th} islands is given by $\sigma_{i,t}^x \sigma_{j',t}^x$.

while H_J remains invariant.³⁷ Here, the sign of the interaction is determined by gauge bits $s_{i,j} = \pm 1$. The state-space is subjected to the following constraints:

$$\prod_i \sigma_i^z = 1, \quad \prod_w \prod_{\square} s_{ij} = 1, \quad (15)$$

where \prod_w denote the product over all the white plaquettes (see Fig. 3).³⁸ The above constraints arise from the fact that the total fermion number parity of all the islands is conserved. The spectrum of the Hamiltonian in Eq. (3) is given by the union of the spectra of Eq. (14) for different gauge bit configurations. Here, gauge bit configurations are nonequivalent if their product around any plaquette differs.³⁹ The Hamiltonian is invariant under the simultaneous transformations U_θ :

$$e^{i\phi_i} \mapsto e^{i\phi_i} e^{i\theta}, \quad \sigma_i^+ \mapsto \sigma_i^+ e^{i\theta/2}. \quad (16)$$

Physically, this global symmetry originates from the fact that the spins correspond to single-electrons that carry half of the charge of the Cooper pairs.

The different phases of the system arise depending on how H_C , H_M or H_J break the $U(1)$ symmetry.¹⁵ In the phase when the Josephson tunneling is the strongest, the $U(1)$ symmetry is spontaneously broken, the rotors align and the ground state of the system is invariant under rotation by multiples of 2π . Then, the system is a conventional superconductor of Cooper pairs (of charge $2e$). We denote this phase by $\{2\pi\}$. When the Majorana-assisted single electron tunneling is the strongest, the $U(1)$ symmetry is again broken. However, now the spins are aligned and the ground state is invariant only under

rotation by multiples of 4π . Moreover, the alignment of the spins in turn aligns the rotors. As a result, the system is an ‘exotic’ superconductor^{21–23} of charge- e bosons. We denote this phase by $\{4\pi\}$. Finally, when the charging energy is the strongest, the complete $U(1)$ is restored, the rotors and the spins are disordered and the system is a Mott insulator. We denote this phase by $\{\theta\}$.

The relevant field theory capturing the phase-diagram of this system was proposed in Ref. 15. In the next section, we compute the one-loop correction to the field theory describing the transition between the phases $\{\theta\}$ and $\{2\pi\}$. Our calculation shows that an additional tricritical point is likely to be present in the phase-diagram which was not captured by the mean-field analysis of Ref. 15.

V. ONE LOOP CORRECTION TO THE FIELD THEORY

Consider the coarse-grained expectation values of $e^{i\phi_i}$ and σ_i^+ in imaginary time τ , denoted by complex fields $\psi_r(\mathbf{r}, \tau)$ and $\psi_s(\mathbf{r}, \tau)$. The relevant degrees of freedom are given by the low-frequency, long-wavelength behavior of these complex fields. The microscopic symmetry U_θ is elevated to the symmetry $\psi_r \mapsto \psi_r e^{i\theta}$, $\psi_s \mapsto \psi_s e^{i\theta/2}$ on the coarse-grained variable that has to be respected in the effective field theory. Since close to the phase transitions, the fields are small, the action can be expanded in a Taylor and gradient expansion in ψ_r, ψ_s . The partition function at zero temperature is given by $Z = \int \mathcal{D}\psi_s \mathcal{D}\psi_s^* \mathcal{D}\psi_r \mathcal{D}\psi_r^* e^{-S}$ with the Euclidean action

$$S = \int d^2r d\tau \left[|\partial_\tau \psi_s|^2 + |\partial_\tau \psi_r|^2 + K_s |\nabla \psi_s|^2 + K_r |\nabla \psi_r|^2 + r_M |\psi_s|^2 + r_J |\psi_r|^2 + u_s |\psi_s|^4 + u_r |\psi_r|^4 + \beta |\psi_s|^2 |\psi_r|^2 - \alpha (\psi_s^{*2} \psi_r + \psi_s^2 \psi_r^*) \right]. \quad (17)$$

The parameter r_x is used to tune through the phase transition and corresponds to $-E_x/E_C$, where $x = M, J$. From stability considerations, u_s, u_r, β must be positive and we choose $\alpha > 0$ without loss of generality.

The phase transition between the phases $\{\theta\}$ and $\{2\pi\}$ is the conventional Mott-insulator to superconductor transition.^{16,19,20} Across this transition, ψ_s stays zero, while $|\psi_r|$ turns finite. Integrating over small fluctuations $\delta\psi_s$ around the saddle point $\bar{\psi}_s = 0$, we get an effective partition function $Z^{(b)} = \int \mathcal{D}\psi_r \mathcal{D}\psi_r^* e^{-S^{(b)}}$ with¹⁵

$$S^{(b)} = \int d^2r d\tau \left[|\partial_\tau \psi_r|^2 + K_r |\nabla \psi_r|^2 + r_J |\psi_r|^2 + u_r |\psi_r|^4 \right].$$

Here, we have kept the renormalization of the couplings to zeroth order in α, β . The phase transition line is given by $r_J = 0$ and it becomes metastable in the phase $\{4\pi\}$. Next, we perform calculations going beyond the zeroth order in α, β . We show that due to the cubic term proportional to α in Eq. (17), this line of phase transition also terminates in a tricritical point. After this point, the

transition turns first order. For the ease of computation, we define $\mathbf{x} = (\mathbf{r}, \tau)$ and rescale the spatial axis so as to set $K_s = 1$. The rescaled stiffness of the rotor sector is denoted by \tilde{K}_r .

Considering small-fluctuations around the saddle point: $\psi_s = \bar{\psi}_s + \delta\psi_s$ and expanding to second order, the effective action can be written as

$$S^{(b)} = S[\delta\psi_s] + S[\psi_r] + S[\delta\psi_s, \psi_r] \quad (18)$$

where the actions for the spin and rotor fields are given by:

$$S[\delta\psi_s] = \int_x \left\{ |\partial_\tau \delta\psi_s|^2 + |\nabla \delta\psi_s|^2 + r_M |\delta\psi_s|^2 \right\},$$

$$S[\psi_r] = \int_x \left\{ |\partial_\tau \psi_r|^2 + \tilde{K}_r |\nabla \psi_r|^2 + r_J |\psi_r|^2 + u_r |\psi_r|^4 \right\},$$

while the interaction between the two is given by

$$S[\delta\psi_s, \psi_r] = \int_x \left\{ -\alpha (\delta\psi_s^{*2} \psi_r + \delta\psi_s^2 \psi_r^*) + \beta |\delta\psi_s|^2 |\psi_r|^2 \right\}.$$

Here, $\int_x \equiv \int d^3x$. Now, the field $\delta\psi_s$ can be perturbatively integrated out. The diagrams contributing to the renormalization of the action to one loop order are shown in Fig. 4.

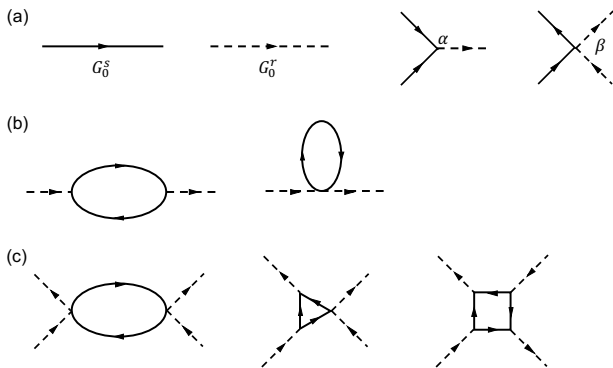


FIG. 4. (a) The solid (dashed) line corresponds to the propagator for the $\psi_{s(r)}$ field. The relevant nonlinear interaction vertices coupling ψ_s, ψ_r are shown. The three (four) point vertex corresponding to the cubic (quartic) interaction with coupling strength $\alpha(\beta)$. (b) Diagrams contributing to the renormalization of the propagator of the ψ_r field. (c) Diagrams contributing to the renormalization of the interaction term $u_r |\psi_r|^4$.

Thus, the effective action for the rotor field is given by

$$S[\psi_r] = \int_x \left\{ (1 + \delta\tilde{K}_r) |\partial_\tau \psi_r|^2 + (\tilde{K}_r + \delta\tilde{K}_r) |\nabla \psi_r|^2 \right. \\ \left. + (r_J + \delta r_J) |\psi_r|^2 + (u_r + \delta u_r) |\psi_r|^4 \right\},$$

where

$$\delta\tilde{K}_r = 4\alpha^2 \int_p \frac{1}{(r_M + p^2)^3}$$

$$\delta r_J = -4\alpha^2 \int_p \frac{1}{(r_M + p^2)^2} + \beta \int_p \frac{1}{(r_M + p^2)}$$

$$\delta u_r = -\frac{\beta^2}{2} \int_p \frac{1}{(r_M + p^2)^2} + 4\alpha^2 \beta \int_p \frac{1}{(r_M + p^2)^3}$$

$$- 144\alpha^4 \int_p \frac{1}{(r_M + p^2)^4}, \quad (19)$$

where $\int_p = \int \frac{d^3p}{(2\pi)^3}$. Note that there are no infrared singularities in these diagrams since $r_M \neq 0$ as we are far from the phase-transition in the spin-sector. The renormalization of the spin-wave stiffness $\delta\tilde{K}_r$ can be evaluated to be:

$$\delta\tilde{K}_r = \frac{1}{8\pi} \frac{\alpha^2}{r_M^{3/2}} \quad (20)$$

The renormalization of the gap-parameter δr_J has the usual cut-off-dependent shift as is common in one-loop renormalization group analysis:

$$\delta r_J = -\frac{\alpha^2}{2\pi r_M^{1/2}} - \frac{\beta r_M^{1/2}}{4\pi} + \frac{\beta r_M^{1/2}}{2\pi^2} \Lambda, \quad (21)$$

where Λ is the ultraviolet cut-off. Finally, the renormalization of u_r is given by:

$$\delta u_r = -\frac{1}{16\pi} \frac{\beta^2}{r_M^{1/2}} + \frac{1}{8\pi} \frac{\alpha^2 \beta}{r_M^{3/2}} - \frac{9}{4\pi} \frac{\alpha^4}{r_M^{5/2}}. \quad (22)$$

For large α , $\delta u_r < 0$. Also, for both large and small values of r_M , $\delta u_r < 0$. Thus, without fine-tuning, for generic parameter choices, $\delta u_r < 0$. This implies that the stabilizing quartic interaction is depressed. Thus, it is likely that this line of 3D-XY phase-transition also terminates in a tricritical point. Then, a sextic term generated from integrating out the ψ_s field stabilizes the theory. After the tricritical point, the transition turns first order. The phase-diagram¹⁵, including the additional tricritical point TP₃, is shown in Fig. 5.

VI. CONDUCTIVITIES AT THE DIFFERENT PHASE-TRANSITIONS

In this section, we investigate the charge-response signatures of the different continuous phase-transitions of our model. As discussed in the previous section, the transition between the phases $\{\theta\}$ and $\{2\pi\}$ is of 3D-XY type, which likely terminates in a 3D-XY tricritical point. The same was shown to be true for the transition between the phases $\{\theta\}$ and $\{4\pi\}$.¹⁵ The universal value of conductivity across the 3D-XY phase-transition lines has been calculated analytically using 1/N expansion²⁴

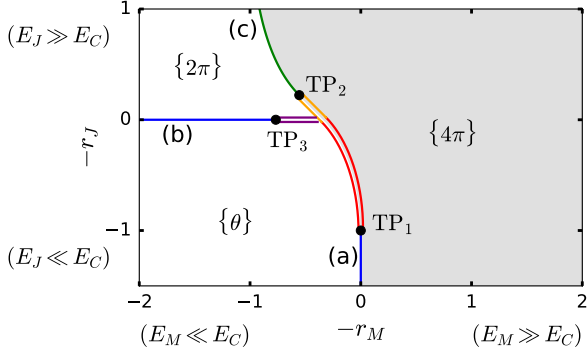


FIG. 5. (Color online) Phase diagram for the model¹⁵ as a function of r_J, r_M for $u_s = u_r = \alpha = \beta = 1$. The blue line, marked with (a), denotes a (2+1)D-XY phase transition line, separating the phases $\{\theta\}$ and $\{4\pi\}$. This transition terminates in a tricritical point (TP₁), after which the transition becomes a first-order transition (shown as red double line). The blue line, marked with (b), also denotes a (2+1)D-XY phase transition line, that separates the phases $\{\theta\}$ and $\{2\pi\}$. This transition line terminates at the tricritical point TP₃, after which the transition turns first order (shown as purple double line). The tricritical point TP₃ is predicted from the one-loop calculations of this work and was missed in the earlier mean-field predictions of Ref. 15. The first order line out of TP₃ meets the first-order line coming out of TP₁. The green line, marked with (c), denotes a (2+1)D-Ising transition line separating the phases $\{2\pi\}$ and $\{4\pi\}$. This phase transition line terminates in a tricritical point (TP₂), after which turns into a first-order line (shown as orange double line), which smoothly transforms into the red first-order line.

and ϵ expansion²⁵. These results can be directly applied for the 3D-XY transitions of our model and the 3D-XY tricritical points. On the other hand, a 3D-Ising line terminating at a 3D-Ising tricritical point separates the the phases $\{2\pi\}$ and $\{4\pi\}$. The charge response across this transition has not been analyzed before. We do this calculation using $1/N$ expansion.

In what follows, first, we summarize the results for the 3D-XY transitions. Since we need the $1/N$ formalism for the subsequent calculation, we sketch the details in the context of the 3D-XY transitions. Then, we perform the relevant analysis for the 3D-Ising transition. Finally, we provide the conductivities across the different tricritical points.

The Kubo formula for the conductivity is given by^{20,40}

$$\sigma_{xx}(ik_z) = \frac{\hbar}{k_z} \int d^3x e^{i\mathbf{k}\cdot\mathbf{x}} \frac{\delta^2 F}{\delta A_x(\mathbf{x}) \delta A_x(0)} \Big|_{\mathbf{A}=0}, \quad (23)$$

where $\mathbf{x} = (\mathbf{r}, \tau)$, $\mathbf{k} = (0, 0, k_z)$ and $F = -\ln Z$. The coupling to the electromagnetic field is performed by making the previously encountered global U(1) symmetry, denoted by angle θ [cf. Eq. (16)], a local one, *i.e.*, space-time dependent: $\theta \rightarrow \theta(\mathbf{r}, \tau)$. Thus, Z can be obtained from the earlier action given by Eq. (17) after the minimal substitution: $\nabla \psi_{s,r} \rightarrow (\nabla - i \frac{e_{s,r}}{\hbar} \mathbf{A}) \psi_{s,r}$.

Here, e_s and e_r are the charges of the spin and rotor fields and are given by e and $2e$ respectively. This is because while the rotor sector conducts electric current via Cooper pairs, the spin sector, arising out of the Majorana zero modes, conduct current through single electrons. The DC-conductivity is obtained by first analytically continuing our result to $ik_z \rightarrow \omega + i0^+$, followed by taking the limit of $\omega \rightarrow 0$ (see Chap. 3 of Ref. 40). The electric current is carried by both spin and rotor current fields, given by

$$\mathbf{J}_{s(r)}(\mathbf{x}) = \frac{1}{2i} \{ \psi_{s(r)}^*(\mathbf{x}) \nabla \psi_{s(r)}(\mathbf{x}) - \psi_{s(r)}(\mathbf{x}) \nabla \psi_{s(r)}^*(\mathbf{x}) \}. \quad (24)$$

From Eq. (23), we get:

$$\sigma_{xx}(ik_z) = \frac{e_s^2}{\hbar} \frac{\rho_s(k_z)}{k_z} + \frac{e_r^2}{\hbar} \frac{\rho_r(k_z)}{k_z} - \frac{4e_s e_r}{\hbar} \frac{\rho_{sr}(k_z)}{k_z}, \quad (25)$$

where

$$\rho_{s(r)}(k_z) = 2 \langle \psi_{s(r)}^*(0) \psi_{s(r)}(0) \rangle - 4 \int d^3x \langle \mathbf{J}_{s(r),x}(\mathbf{x}) \mathbf{J}_{s(r),x}(0) \rangle e^{i\mathbf{k}\cdot\mathbf{x}}, \quad (26)$$

$$\rho_{sr}(k_z) = \int d^3x \{ \langle \mathbf{J}_{s,x}(\mathbf{x}) \mathbf{J}_{r,x}(0) \rangle + \langle \mathbf{J}_{r,x}(\mathbf{x}) \mathbf{J}_{s,x}(0) \rangle \} e^{i\mathbf{k}\cdot\mathbf{x}}. \quad (27)$$

A. Conductivities at the 3D-XY transitions

Consider the 3D-XY transition between the phases $\{\theta\}$ and $\{4\pi\}$ [line (a) in Fig. 5]. The relevant action is given by¹⁵

$$S^{(a)} = \int d^3x \left\{ |\partial_\tau \psi_s|^2 + K_s |\nabla \psi_s|^2 + r_M |\psi_s|^2 + \frac{u_M}{2} |\psi_s|^4 + \tilde{u}_M |\psi_s|^6 \right\}. \quad (28)$$

For the $u_M > 0$, the transition is of the 3D-XY type and the sextic term can be neglected.⁴¹ We will treat this case in this subsection. The tricritical points are treated in Sec. VI C. We perform perturbation in the inverse of the dimensionality of the order parameter N .^{24,42–44} For this case, with complex order parameter, $N = 2$. The effective action in terms of the N -component order parameter is given by

$$S_{\text{eff}}^{(a)} = \int d^3x \left\{ \nabla \psi_{s,\alpha}^* \nabla \psi_{s,\alpha} + r_M \psi_{s,\alpha}^* \psi_{s,\alpha} + \frac{u_M}{2} (\psi_{s,\alpha}^* \psi_{s,\alpha})^2 \right\}, \quad (29)$$

where ∇ now denotes the 3D gradient. We have rescaled the spatial axis so as to set $K_s = 1$. We consider N' complex fields, $\psi_{s,\alpha}$, $\alpha = 1, \dots, N'$, where $N = 2N'$.

For this effective field theory, the conductivity is given by

$$\sigma_{xx}(ik_z) = \frac{e_s^2}{\hbar} \frac{\rho_s(k_z)}{k_z}, \quad (30)$$

where $\rho_s(k_z)$ is defined in Eq. (26) after the transformation: $\psi_s \rightarrow \psi_{s,\alpha}$. The current operator is defined by Eq. (24) after the same transformation. We define the Fourier transform of $\psi_{s,\alpha}$:

$$\psi_{s,\alpha}(\mathbf{x}) \equiv \frac{1}{\sqrt{\Omega}} \sum_{\mathbf{q}} e^{i\mathbf{q}\cdot\mathbf{x}} \psi_{s,\alpha}(\mathbf{q}), \quad (31)$$

where Ω is the 3D volume element. In Fourier domain, the effective action is given by

$$S_{\text{eff}}^{(a)} = \sum_{\mathbf{q}} (\mathbf{q}^2 + r_M) \psi_{s,\alpha}^*(\mathbf{q}) \psi_{s,\alpha}(\mathbf{q}) + \frac{1}{2\Omega} \sum_{\mathbf{q}} u_M \sum_{\mathbf{p}, \mathbf{p}'} \psi_{s,\alpha}^*(\mathbf{p} + \mathbf{q}) \psi_{s,\beta}^*(\mathbf{p}') \psi_{s,\alpha}(\mathbf{p}) \psi_{s,\beta}(\mathbf{p}' + \mathbf{q}) \}. \quad (32)$$

The expression for $\rho_s(k_z)$ is given by:

$$\rho_s(k_z) = \frac{2}{\Omega} \sum_{\mathbf{q}} \langle \psi_{s,\alpha}^*(\mathbf{q}) \psi_{s,\alpha}(\mathbf{q}) \rangle - \frac{4}{\Omega} \sum_{\mathbf{p}, \mathbf{q}} q_x p_x \langle \psi_{s,\alpha}^*(\mathbf{q} - \mathbf{k}/2) \psi_{s,\alpha}^*(\mathbf{p} + \mathbf{k}/2) \psi_{s,\alpha}(\mathbf{p} - \mathbf{k}/2) \psi_{s,\alpha}(\mathbf{q} + \mathbf{k}/2) \rangle. \quad (33)$$

Since in three dimensions, the quartic coupling is relevant, we treat it perturbatively using the $1/N$ -expansion. To obtain a non-trivial result, we must choose $u_M = g_M/N$, where g_M stays constant. Following Ref. 43, we can decouple the interaction by Hubbard-Stratonovich transformation, introducing an auxiliary field $\zeta(\mathbf{r})$, leading to an effective action:

$$S_{\text{eff}}^{(a)}[\psi_{s,\alpha}, \zeta] = \int d^3x \left\{ \nabla \psi_{s,\alpha}^* \nabla \psi_{s,\alpha} + r_M \psi_{s,\alpha}^* \psi_{s,\alpha} + \frac{N}{2g_M} \zeta^2 + i\zeta \psi_{s,\alpha}^* \psi_{s,\alpha} \right\}. \quad (34)$$

The linear term in the above action can be removed by shifting the ζ field: $\zeta \rightarrow \zeta + \bar{\zeta}$, where $\bar{\zeta}$ is determined by

$$\left. \frac{\partial \tilde{S}_{\text{eff}}^{(a)}[\zeta]}{\partial \zeta} \right|_{\zeta=\bar{\zeta}} = 0, \quad (35)$$

with

$$e^{-\tilde{S}_{\text{eff}}^{(a)}[\zeta]} = \int \mathcal{D}\psi_{s,\alpha} \mathcal{D}\psi_{s,\alpha}^* e^{-S_{\text{eff}}^{(a)}[\psi_{s,\alpha}, \zeta]}. \quad (36)$$

The action then becomes

$$S_{\text{eff}}^{(a)}[\psi_{s,\alpha}, \zeta] = \int d^3x \left\{ \nabla \psi_{s,\alpha}^* \nabla \psi_{s,\alpha} + \tilde{r}_M \psi_{s,\alpha}^* \psi_{s,\alpha} + \frac{N}{2g_M} \zeta^2 + i\zeta \psi_{s,\alpha}^* \psi_{s,\alpha} + \frac{N}{g_M} \bar{\zeta} \zeta \right\}, \quad (37)$$

where $\tilde{r}_M = r_M + i\bar{\zeta}$, is the renormalized gap parameter that goes to zero at the phase-transition. The last two terms cancel, thereby eliminating the linear term in ζ . The free propagator for the $\psi_{s,\alpha}$ field is given by

$$G_0^\psi(\mathbf{q}) = \frac{1}{\mathbf{q}^2 + \tilde{r}_M} \quad (38)$$

and the resummed two-body interaction mediated by the ζ is given by

$$\tilde{u}_M(\mathbf{k}) = \frac{u_M}{1 + u_M N' \Pi^\psi(\mathbf{k})}, \quad (39)$$

where

$$\Pi^\psi(\mathbf{k}) = \int \frac{d^3q}{(2\pi)^3} G_0^\psi(\mathbf{k} + \mathbf{q}) G_0^\psi(\mathbf{q}). \quad (40)$$

Note that as $N' \rightarrow \infty$, the effective action is free with $\tilde{u}_M \rightarrow 0$. The $1/N$ -expansion can now be performed by replacing r_M, u_M by $\tilde{r}_M, \tilde{u}_M(\mathbf{k})$. The details of the calculation can be found in Ref. 24. Here, we merely state the result:

$$\sigma_{xx} = \frac{\pi}{8} \left(1 - \frac{1}{N'} \frac{32}{9\pi^2} \right) \frac{e^2}{h} = \frac{\pi}{8} \left(1 - \frac{32}{9\pi^2} \right) \frac{e^2}{h}, \quad (41)$$

where in the last equality, we have set $N' = 1$ for the 3D-XY transition.

For the phase-transition between the $\{\theta\}$ and the $\{2\pi\}$ phases [line (b) in Fig. 5], the same calculation can be performed, with the following substitution: $e_s \rightarrow e_r = 2e$. Thus, in that case, the DC-conductivity is given by

$$\sigma_{xx} = \frac{\pi}{2} \left(1 - \frac{32}{9\pi^2} \right) \frac{e^2}{h}. \quad (42)$$

B. Conductivity at the 3D-Ising transition

For the effective action for the transition between $\{2\pi\}$ and $\{4\pi\}$ [line (c) in Fig. 5], we use the parametrization¹⁵

$$\psi_r = (\bar{\rho}_r + \delta\rho_r) e^{i\theta_r/\bar{\rho}_r}, \quad (43)$$

$$\psi_s = (\sigma + iw) e^{i\theta_r/2\bar{\rho}_r} \quad (44)$$

where $\bar{\rho}_r$ is the saddle point value of $|\psi_r|$ and the real fields $\delta\rho_r, \theta_r$ and σ, w denote the fluctuations of $\delta\psi_r$ and

$\delta\psi_s$. The fluctuations in θ_r correspond to the massless Goldstone mode associated with the symmetry breaking in the rotor sector. They decouple from the rest. As described in Ref. 15, the emergent Ising degree of freedom σ undergoes the transition, while the fields $w, \delta\rho_r$ stay regular with gap parameters $r_w, r_{\delta\rho_r} > 0$. The effective action for the Ising degree of freedom is given by

$$S^{(c)} = \int d^3x \{ (\partial_\tau \sigma)^2 + K_s (\nabla \sigma)^2 + t_c \sigma^2 + \frac{u_c}{2} \sigma^4 + \tilde{u}_c \sigma^6 \}. \quad (45)$$

Again, in this subsection, we consider the case when $u_c > 0$ (see Sec. VI C for $u_c = 0$). In this new parametrization, the electric current is carried by [using Eq. (24) and Eqs. (43,44)]

$$\mathbf{J}_s = \sigma \nabla w - w \nabla \sigma + \frac{\sigma^2 + w^2}{2\bar{\rho}_r} \nabla \theta_r, \quad (46)$$

$$\mathbf{J}_r = \frac{(\bar{\rho}_r + \delta\rho_r)^2}{\bar{\rho}_r} \nabla \theta_r. \quad (47)$$

Defining Fourier transforms as in Eq. (31) for $\sigma, w, \delta\rho_r$ and θ_r , we can write the effective action in Fourier domain. From Eq. (45), the action for the σ -field, undergoing the Ising transition, is given by

$$S[\sigma] = \sum_{\mathbf{q}} (\mathbf{q}^2 + t_c) \sigma(\mathbf{q}) \sigma(-\mathbf{q}) + \frac{1}{2\Omega} \sum_{\mathbf{p}} u_c \sum_{\mathbf{q}, \mathbf{q}'} \sigma(\mathbf{q}) \sigma(\mathbf{q}') \sigma(\mathbf{p} - \mathbf{q}') \sigma(-\mathbf{p} - \mathbf{q}'). \quad (48)$$

Since the fields $w, \delta\rho_r, \theta$ remain regular, we only need the action governing them to quadratic order. The action for the w -field is given by

$$S[w] = \sum_{\mathbf{q}} (\mathbf{q}^2 + r_w) w(\mathbf{q}) w(-\mathbf{q}), \quad (49)$$

The mean-field form of r_w is given by¹⁵

$$r_w = r_M + \alpha \sqrt{\frac{-2r_J}{u_r}} - \frac{\beta r_J}{2u_r} \quad (50)$$

$$= \alpha \sqrt{\frac{-8r_J}{u_r}}, \quad (51)$$

where the last line is valid only on the Ising-transition line. The actions for $\delta\rho_r$ and θ_r are given by the Gaussian actions:

$$S[\delta\rho_r] = \sum_{\mathbf{q}} [q_z^2 + \tilde{K}_r (q_x^2 + q_y^2) + r_{\delta\rho_r}] \delta\rho_r(\mathbf{q}) \delta\rho_r(-\mathbf{q}),$$

$$S[\theta_r] = \sum_{\mathbf{q}} [q_z^2 + \tilde{K}_r (q_x^2 + q_y^2)] \theta_r(\mathbf{q}) \theta_r(-\mathbf{q}), \quad (52)$$

where $r_{\delta\rho_r} = -2r_J > 0$ in terms of the bare action parameters.

To compute the conductivity, we again resort to a perturbation based on the $1/N$ -expansion. Much of the earlier formalism can be borrowed over to the real fields.^{43,44}

We consider an N -component σ_α field. Doing again a Hubbard-Stratonovich decoupling and resumming the bubble-diagrams, we get the effective free-field propagator for the σ_α field:

$$G_0^\sigma(q) = \frac{1}{2(\mathbf{q}^2 + \tilde{t}_c)}, \quad (53)$$

where \tilde{t}_c is the renormalized gap-parameter that goes to zero at the phase-transition. The effective interaction is given by

$$\tilde{u}_c(\mathbf{k}) = \frac{u_c}{1 + u_c N \Pi^\sigma(\mathbf{k})}, \quad (54)$$

where now,

$$\Pi^\sigma(\mathbf{k}) = \int \frac{d^3q}{(2\pi)^3} G_0^\sigma(\mathbf{k} + \mathbf{q}) G_0^\sigma(\mathbf{q}). \quad (55)$$

To perform the $1/N$ computation, we replace t_c, u_c by $\tilde{t}_c, \tilde{u}_c(\mathbf{k})$ and evaluate Eq. (25). We drop the flavor indices from now on. As will be shown below, the superconducting density changes as the system undergoes the Ising phase transition from $\{2\pi\}$ to the $\{4\pi\}$ phases. This change depends on the gap parameter of the w -field. Hence, it is non-universal and depends on the superconducting density before the transition. Thus, we restrict ourselves only to the lowest non-vanishing order in $1/N$ expansion.

To the lowest (zeroth) order in $1/N$, we set $\tilde{u}_c(\mathbf{k})$ to zero resulting in a Gaussian theory for all the fields. First, we calculate the contribution to the conductivity from $\rho_s(k_z)$. In the current parametrization, from Eq. (26), one gets

$$\rho_s^{(0)}(k_z) = \frac{2}{\Omega} \sum_{\mathbf{q}} \{ \langle \sigma(\mathbf{q}) \sigma(-\mathbf{q}) \rangle + \langle w(\mathbf{q}) w(-\mathbf{q}) \rangle \}$$

$$- \frac{8}{\Omega} \sum_{\mathbf{p}, \mathbf{q}, \mathbf{q}'} \langle \sigma(\mathbf{p}) \sigma(\mathbf{q}) w(-\mathbf{k} - \mathbf{p}) w(\mathbf{q}') \rangle p_x (q'_x - q_x),$$

where we have used the definition of \mathbf{J}_s [cf. Eq. (46)], the fact that $\langle \theta_r(\mathbf{q}) \rangle = 0$ and neglected terms of the order $1/\bar{\rho}_r^2$. By making the last approximation, we restrict ourselves to the regime where the phase $\{2\pi\}$ is sufficiently well-developed (recall that in terms of mean-field estimates, $\bar{\rho}_r = \sqrt{-r_J/2u_r}$). Using the expressions for the propagators for σ, w , we get

$$\rho_s^{(0)}(k_z) = \int \frac{d^3q}{(2\pi)^3} \left[\frac{1}{\tilde{t}_c + \mathbf{q}^2} + \frac{1}{r_w + \mathbf{q}^2} - \frac{4q_x^2}{(\tilde{t}_c + \mathbf{q}^2) \{ r_w + (\mathbf{k} + \mathbf{q})^2 \}} \right] \quad (56)$$

Using the result²⁴ that

$$\int \frac{d^3q}{(2\pi)^3} \frac{\partial}{\partial q_x} [q_x G_0^\sigma(q)] = 0, \quad (57)$$

one can rewrite Eq. (56) at the critical point as⁴⁵

$$[\rho_s^{(0)}(k_z)]_{\text{crit}} = \int \frac{d^3q}{(2\pi)^3} \frac{2q_x^2}{\mathbf{q}^2} \left[\frac{1}{r_w + \mathbf{q}^2} - \frac{2}{r_w + (\mathbf{q} + \mathbf{k})^2} \right]. \quad (58)$$

The above integral can be evaluated exactly. After some algebra, we get

$$\frac{[\rho_s^0(ik_z \rightarrow \omega + i0^+)]_{\text{crit}}}{k_z} = \frac{\sqrt{r_w}}{6\pi} \frac{i}{\omega + i0^+}. \quad (59)$$

Upon taking the real part of this above equation, we find that this gives rise to a superconducting response with superconducting density $\delta n_s = \sqrt{r_w}/6\pi$.

Next, we compute the contributions to conductivity from ρ_{sr} and ρ_r . Since $\mathbf{k} = (0, 0, k_z)$, it follows that

$$\int d^3e^{i\mathbf{k}\cdot\mathbf{x}} \langle \partial_x \theta_r(\mathbf{x}) \partial_x \theta_r(0) \rangle = 0. \quad (60)$$

This implies $\rho_{sr} = 0$. Finally, the contribution to conductivity from $\rho_r(k_z)$ is the usual superconducting response. It can be computed analogously and to leading order (deep in the $\{2\pi\}$ phase) is given by

$$\rho_r^{(0)}(k_z) = 2\bar{\rho}_r^2. \quad (61)$$

Thus, the total contribution to the real part of the conductivity is given by

$$\text{Re}[\sigma_{xx}] = \frac{\pi e^2}{\hbar} (\bar{n}_s + \delta n_s) \delta(\omega), \quad (62)$$

where the first contribution $\bar{n}_s = 8\bar{\rho}_r^2$ comes from the superconducting density due to the usual superconductivity. The second denoted by $\delta n_s = \sqrt{r_w}/6\pi$ is the renormalization of the superconducting density due to the Ising transition. An estimate of the gap parameter for the w field is obtained by replacing ψ_r by $\bar{\rho}_r$ in the action of Eq. (17) with the parametrization of Eqs. (43) and (44). Then, $r_w = 2\alpha\bar{\rho}_r$. Thus, the fractional change in the superconducting density is given by:

$$\frac{\delta n_s}{\bar{n}_s} = \frac{2}{3\pi} \left(\frac{\alpha}{\bar{n}_s^3} \right)^{1/2}. \quad (63)$$

The above equation relates the change in the superconducting density with the coupling constant α and provides the following two important insights. Firstly, the cubic coupling can be measured by measuring the change in the superconducting density as one tunes through the Ising phase transition. A larger jump in the density indicates a larger cubic coupling and vice versa. Secondly, it also provides an estimate of the change in the superconducting density as the Josephson coupling changes. It follows from Eq. (63) that as one increases the Josephson coupling, the change in the superconducting density decreases. This is because \bar{n}_s increases⁴⁶.

C. Conductivities at the tricritical points

We conclude this section by briefly addressing the conductivities at the Ising and XY tricritical points. The upper critical dimension for the sextic interaction is three. Therefore, modulo logarithmic corrections because of the interaction being marginal, the universal quantities are given by the effective Gaussian theories. Thus, the results from the previous sections can be directly applied.

For the 3D-XY tricritical point separating phases $\{\theta\}$ and $\{4\pi\}$ (TP₁ in Fig. 5), the conductivity can be obtained by setting $N \rightarrow \infty$ (see Ref. 24 for details). Therefore, the conductivity at this point is given by

$$\sigma_{xx} = \frac{\pi e^2}{8 \hbar}. \quad (64)$$

Thus, the conductivity increases along the 3D-XY line and approaches the above value from the one given by Eq. (42) as one approaches the tricritical point. Similarly, the conductivity at the tricritical point separating phases $\{\theta\}$ and $\{2\pi\}$ (TP₃ in Fig. 5), the conductivity is given by

$$\sigma_{xx} = \frac{\pi e^2}{2 \hbar}. \quad (65)$$

At the 3D-Ising tricritical point (TP₂ in Fig. 5), the conductivity is given by Eq. (62). As discussed earlier, there is no dissipative component to the conductivity. Only the superconducting density changes across the transition. The change is largest at the tricritical point and decreases along the Ising phase-transition line.

VII. CONCLUSION

To summarize, we have presented in this paper the charge-response of the Majorana toric code. From the basic microscopic Hamiltonian, after a Jordan-Wigner transformation, we mapped the problem to that of spins coupled to rotors. We computed a correction to the previously proposed field theory to one-loop order. Our calculations show that the phase-diagram is likely to contain another tricritical point of the 3D-XY type. Subsequently, we computed the conductivities at the different continuous phase-transitions using $1/N$ expansion. We provided the universal conductivities at the two 3D-XY phase-transitions and at the 3D-XY tricritical point. Next, we calculated the change in the superconducting density as the system undergoes the 3D-Ising phase-transition from a charge- $2e$ to a charge- e superconductor. We showed that the change in the superconducting density provides an estimate of the nonlinear coupling between the spin and rotor fields. We emphasize that the calculated conductivities provide unique signatures of the different phase-transitions in the model. At the two 3D-XY transitions, the system behaves as a metal, where the conductivities have universal values. On the

other hand, for the Ising transition, out of two coupled real fields responsible for carrying the current, only one undergoes a phase-transition. This results in a jump of the superconducting density across the transition. With the recent developments in detecting Majorana bound-states in solid-state systems,^{47,48} we are optimistic of experimental verifications of our field theory predictions.

Discussions with Barbara Terhal and David DiVincenzo are gratefully acknowledged. AR acknowledges the support through the ERC Consolidator Grant No. 682726 and the Alexander von Humboldt foundation. FH acknowledges the support of the Excellent Initiative of the Deutsche Forschungsgemeinschaft.

Appendix A: Mean-field analysis

In this section, we perform a mean-field calculation that provide supporting evidence for the proposed field theory of Ref. 15. This can be done by first writing a Hubbard-Stratonovich decoupling in path-integral form and solving the corresponding Schrödinger problem^{19,20} using perturbation theory. To that end, we introduce two complex order parameters, ψ_s and ψ_r , respectively for the spin and rotor sectors of our model. Thus, at each lattice site, we define:

$$\sigma_i^+ = \psi_s + (\sigma_i^+ - \psi_s), \quad (\text{A1})$$

$$e^{i\phi_i} = \psi_r + (e^{i\phi_i} - \psi_r). \quad (\text{A2})$$

We perform perturbation analysis with the unperturbed Hamiltonian H_C . Expanding around these order parameters and keeping to leading order, the mean field perturbation Hamiltonian is:

$$\begin{aligned} H_M^{\text{mf}} + H_J^{\text{mf}} = & -zE_M \sum_i \left\{ [2\psi_s^* \psi_r + \psi_s(1 + |\psi_r|^2)] \sigma_i^- \right. \\ & \left. + (\psi_s^2 + |\psi_s|^2 \psi_r) e^{-i\phi_i} + \text{H.c.} \right\} \\ & - zE_J \sum_i (\psi_r e^{-i\phi_i} + \text{H.c.}), \end{aligned} \quad (\text{A3})$$

where $z = 4$ is the number of nearest neighbors around each lattice point. Since the order parameters are independent of the site index, the problem effectively reduces to that of a single site. Hence, we drop the site index. The ground state energy per site of the total interacting Hamiltonian can be written as:

$$\begin{aligned} \frac{E_g}{N_{\text{tot}}} = & \frac{E_{\text{mf}}}{N_{\text{tot}}} - zE_M [\langle \sigma^- \rangle^2 \langle e^{i\phi} \rangle + \langle \sigma^+ \rangle^2 \langle e^{-i\phi} \rangle] \\ & + \langle \sigma^+ \rangle \langle \sigma^- \rangle (1 + \langle e^{i\phi} \rangle \langle e^{-i\phi} \rangle) - zE_J \langle e^{i\phi} \rangle \langle e^{-i\phi} \rangle \\ & + zE_C [v_1 \langle \sigma^- \rangle + v_1^* \langle \sigma^+ \rangle + v_2 \langle e^{-i\phi} \rangle + v_2^* \langle e^{i\phi} \rangle]. \end{aligned}$$

Here E_g is the total ground state energy, N_{tot} is the number of lattice sites, E_{mf} is the energy of the mean field

model calculated using perturbation theory and

$$\begin{aligned} v_1 = & \frac{E_M}{E_C} [2\psi_s^* \psi_r + \psi_s(1 + |\psi_r|^2)], \\ v_2 = & \frac{E_M}{E_C} (\psi_s^2 + |\psi_s|^2 \psi_r) + \frac{E_J}{E_C} \psi_r. \end{aligned} \quad (\text{A4})$$

We perform this computation till fourth order in order to get the relevant terms of the field theory given in Eq. (17). The mean field energy E_{mf} in units of E_C is

$$\begin{aligned} \frac{E_{\text{mf}}}{N_{\text{tot}} E_C} = & -z^2 |v_1|^2 - \frac{z^2 |v_2|^2}{2} + z^4 |v_1|^4 + \frac{7z^4 |v_2|^4}{128} \\ & - \frac{10z^4 |v_1 v_2|^2}{9}, \end{aligned} \quad (\text{A5})$$

The ground state is computed to third order in perturbation theory, the explicit form of which is not shown for brevity. Collecting all the terms, one has for the ground state energy:

$$\begin{aligned} \frac{E_g}{N_{\text{tot}} E_C} = & 16 \left(1 - \frac{4E_M}{E_C}\right) |v_1|^2 + 8 \left(1 - \frac{2E_J}{E_C}\right) |v_2|^2 \\ & + 256 |v_1|^4 + \left(6 + \frac{16E_J}{E_C}\right) |v_2|^4 \\ & + \frac{128}{9} \left(-145 + \frac{152E_J}{E_C} + \frac{178E_M}{E_C}\right) |v_1 v_2|^2 \\ & - \frac{128E_M}{E_C} (v_1^2 v_2 + v_1^{*2} v_2^*), \end{aligned} \quad (\text{A6})$$

where we have set $z = 4$. In terms of the order parameters ψ_s, ψ_r , to fourth order, we get

$$\begin{aligned} \frac{E_g}{N_{\text{tot}} E_C} = & \left(1 - \frac{4E_M}{E_C}\right) |\psi_s|^2 + 2 \left(1 - \frac{2E_J}{E_C}\right) |\psi_r|^2 \\ & + 2|\psi_s|^4 + \frac{3}{8} |\psi_r|^4 + 18 |\psi_s|^2 |\psi_r|^2 \\ & + 3(\psi_s^{*2} \psi_r + \psi_s^2 \psi_r^*). \end{aligned} \quad (\text{A7})$$

In the coefficients of the higher than quadratic terms, we have kept only the leading order contributions. The dependence of the ground state energy on the order parameters further justifies the choice of the form of the action argued in Ref. 15 purely on the basis of symmetries. The mean-field estimates of the action parameters are

$$\begin{aligned} r_M = & 1 - \frac{4E_M}{E_C}, \quad r_J = 2 \left(1 - \frac{2E_J}{E_C}\right), \\ u_s = & 2, \quad u_r = \frac{3}{8}, \quad |\alpha| = 3, \quad \beta = 18, \end{aligned} \quad (\text{A8})$$

where we have set the lattice-constant to unity. Therefore, the mean-field estimates of the location of the phase-transition between the $\{\theta\}$ and the $\{4\pi\}$ phases is given by at $E_M = E_C/4$. The same for the phase-transition between the $\{\theta\}$ and the $\{2\pi\}$ phases is $E_J = E_C/2$.

- ¹ D. P. DiVincenzo, *Phys. Scripta* **T137**, 014020 (2009).
- ² A. Kitaev, *Ann. Phys. (NY)* **303**, 2 (2003).
- ³ A. Kitaev, *Ann. Phys. (NY)* **321**, 2 (2006).
- ⁴ A. G. Fowler, M. Mariantoni, J. M. Martinis, and A. N. Cleland, *Phys. Rev. A* **86** (2012), 10.1103/PhysRevA.86.032324.
- ⁵ M. Levin and X.-G. Wen, *Phys. Rev. Lett.* **96**, 110405 (2006).
- ⁶ C. Xu and L. Fu, *Phys. Rev. B* **81**, 1 (2010).
- ⁷ B. M. Terhal, F. Hassler, and D. P. DiVincenzo, *Phys. Rev. Lett.* **108**, 1 (2012).
- ⁸ Z. Nussinov, G. Ortiz, and E. Cobanera, *Phys. Rev. B* **86**, 085415 (2012).
- ⁹ S. Vijay, T. H. Hsieh, and L. Fu, *Phys. Rev. X* **5**, 41038 (2015).
- ¹⁰ L. A. Landau, S. Plugge, E. Sela, A. Altland, S. M. Albrecht, and R. Egger, *Phys. Rev. Lett.* **116**, 1 (2016).
- ¹¹ T. Karzig, C. Knapp, R. M. Lutchyn, P. Bonderson, M. B. Hastings, C. Nayak, J. Alicea, K. Flensberg, S. Plugge, Y. Oreg, C. M. Marcus, and M. H. Freedman, *Phys. Rev. B* **95**, 235305 (2017).
- ¹² D. Litinski, M. S. Kesselring, J. Eisert, and F. Von Oppen, *arXiv:1704.01589* (2017).
- ¹³ A. Yu. Kitaev, *Phys.-Usp.* **44**, 131 (2001).
- ¹⁴ L. Fu, *Phys. Rev. Lett.* **104**, 1 (2010).
- ¹⁵ A. Roy, B. M. Terhal, and F. Hassler, *Phys. Rev. Lett.* **119**, 180508 (2017).
- ¹⁶ M. P. A. Fisher, P. B. Weichman, G. Grinstein, and D. S. Fisher, *Phys. Rev. B* **40**, 546 (1989).
- ¹⁷ R. Fazio and G. Schön, *AIP Conf. Proc.* **427**, 273 (1998).
- ¹⁸ R. Fazio and H. van der Zant, *Phys. Rep.* **355**, 235 (2001).
- ¹⁹ I. Herbut, *A Modern Approach to Critical Phenomena* (Cambridge University Press, 2007).
- ²⁰ S. Sachdev, *Quantum Phase Transitions* (Cambridge University Press, 2011).
- ²¹ X. G. Wen, *Phys. Rev. B* **44**, 2664 (1991).
- ²² L. Balents, M. P. A. Fisher, and C. Nayak, *Phys. Rev. B* **60**, 1654 (1999).
- ²³ T. Senthil and M. P. A. Fisher, *Phys. Rev. B* **62**, 7850 (2000).
- ²⁴ M.-C. Cha, M. P. A. Fisher, S. M. Girvin, M. Wallin, and A. P. Young, *Phys. Rev. B* **44**, 6883 (1991).
- ²⁵ R. Fazio and D. Zappalà, *Phys. Rev. B* **53**, R8883 (1996).
- ²⁶ C. Chamon, R. Jackiw, Y. Nishida, S.-Y. Pi, and L. Santos, *Phys. Rev. B* **81**, 224515 (2010).
- ²⁷ C. W. J. Beenakker, *Phys.Rev.Lett.* **112**, 070604 (2014).
- ²⁸ N. Read and D. Green, *Phys. Rev. B* **61**, 10267 (2000).
- ²⁹ D. A. Ivanov, *Phys. Rev. Lett.* **86**, 268 (2001).
- ³⁰ C. Nayak, S. H. Simon, A. Stern, M. Freedman, and S. Das Sarma, *Reviews of Modern Physics* **80**, 1083 (2008).
- ³¹ C. W. J. Beenakker, *Annual Review of Condensed Matter Physics* **4**, 15 (2013).
- ³² B. van Heck, F. Hassler, A. R. Akhmerov, and C. W. J. Beenakker, *Phys. Rev. B* **84**, 2 (2011).
- ³³ J. Alicea, *Rep. Prog. Phys.* **75**, 076501 (2012).
- ³⁴ Note that for case of $2n$ Majorana zero modes, the remaining topological degeneracy will be 2^{n-1} .
- ³⁵ S. Bravyi, *Phys. Rev. A* **73**, 1 (2006).
- ³⁶ B. van Heck, A. R. Akhmerov, F. Hassler, M. Burrello, and C. W. J. Beenakker, *New J. Phys.* **14**, 035019 (2012).
- ³⁷ Note that while ϕ_i and n_i remain canonically conjugate, n_i now denotes only the excess number of Cooper-pairs on the i -th island.
- ³⁸ Note that $\prod_{\square} s_{ij} = 1$ is trivially true.
- ³⁹ E. Fradkin, *Field Theories of Condensed Matter Physics*, *Field Theories of Condensed Matter Physics* (Cambridge University Press, 2013).
- ⁴⁰ G. Mahan, *Many-Particle Physics*, *Physics of Solids and Liquids* (Springer US, 2013).
- ⁴¹ P. M. Chaikin and T. C. Lubensky, *Principles of Condensed Matter Physics* (Cambridge University Press, 2000).
- ⁴² S.-k. Ma, *Phys. Rev. A* **7**, 2172 (1973).
- ⁴³ S. Coleman, *Aspects of Symmetry: Selected Erice Lectures* (Cambridge University Press, 1988).
- ⁴⁴ J. Zinn-Justin, *Quantum Field Theory and Critical Phenomena*, *International series of monographs on physics* (Clarendon Press, 2002).
- ⁴⁵ We note that Eq. (58) is qualitatively different from the corresponding expression obtained for the 3D-XY transition. In the present case, the complex order parameter is given by $\sigma + iw$, where only σ undergoes a phase transition due to the finite gap r_w . This difference manifests itself in the fact that for finite r_w , $\rho_s^{(0)}$ approaches a constant for $k_z \rightarrow 0$ (corresponding to a superconducting response). On the other hand, for the XY-transition (with $r_w = 0$) the leading term is proportional to k_z (corresponding to a dissipative response).
- ⁴⁶ At some point in the parameter space, \bar{n}_s saturates, but it is outside the validity of our field theory analysis.
- ⁴⁷ V. Mourik, K. Zuo, S. M. Frolov, S. R. Plissard, E. P. a. M. Bakkers, and L. P. Kouwenhoven, *Science* **336**, 1003 (2012).
- ⁴⁸ S. M. Albrecht, A. P. Higginbotham, M. Madsen, F. Kuemmeth, T. S. Jespersen, J. Nyg, P. Krogstrup, and C. M. Marcus, *Nature* **531**, 206 (2016).